Dispersion compensation properties of dual-concentric core photonic crystal fibers

Lihong Han (韩利红)*, Liming Liu (刘立明), Zhongyuan Yu (俞重远), Huijie Zhao (赵慧杰), Xin Song (宋 鑫), Jinhong Mu (牟晋宏), Xiu Wu (吴 秀), Junjie Long (龙俊洁), and Xi Liu (刘 习)

State Key Laboratory of Information Photonics and Optical Communications, Beijing University of Posts and Telecommunications, Beijing 100876, China

**Corresponding author: hanlh.star@gmail.com*

Received July 2, 2013; accepted August 20, 2013; posted online January 8, 2014

The dispersion compensation properties of dual-concentric core photonic crystal fibers are theoretically investigated in this letter. The effects of geometric structure on the dispersion properties of dual-concentric core photonic crystal fibers are carefully studied by finite element method. The first layer of holes around the core area is enlarged in a new manner with the near-core point fixed. Considering the tradeoff among several parameters, results show that the dispersion compensation wavelength and strength can be tuned to desired values by constructing an appropriate design of the geometric structure of photonic crystal fibers.

OCIS codes: 060.5295, 230.2035.
doi: 10.3788/COL201412.010603.

Chromatic dispersion is one of the most important parameters of optical communication system[1]. The increasing use of operating wavelength at 1.55 μm caused by the low-loss window of fibers has resulted in a problem wherein the nonzero chromatic dispersion of silica fibers at this wavelength leads to serious restrictions in optical communications. One of the best approaches to reducing chromatic dispersion is to use dispersion-compensating fibers (DCFs), which show a high value of negative dispersion in optical communication systems[2−4]. Photonic crystal fibers (PCFs) have outstanding properties and great versatility. These materials are very useful for chromatic dispersion management. Obtaining very large dispersion compensate coefficient is possible when dispersion compensation PCFs (DC-PCFs) are used[5−8].

The chromatic dispersion coefficient $D$is used to quantify the amount of chromatic dispersion and can be described as

$$D = \frac{\lambda}{c}\frac{d^2 n_{\text{eff}}}{d\lambda^2}, \tag{1}$$

where λ is the operating wavelength, c is the speed of light in a vacuum, and n_{eff} is the effective indices of the fundamental mode at various wavelengths. Dual-concentric core fibers compensate for chromatic dispersion based on the coupling of the inner mode (i.e., the mode propagating in core region) and the outer mode (i.e., the mode propagating in cladding defect area).

In a dual-concentric core fiber, the fundamental mode is confined in the core region as the inner mode, where the wavelengths are shorter than the phase-matching wavelength λ_0. Subsequently, the fundamental mode switches to the cladding defect area as the outer mode, where the wavelengths are longer than λ_0. Based on Eq. (1), the dual-concentric core fiber shows a large negative dispersion D around the phase-matching wavelength because of the fundamental mode switch. DCF with larger negative dispersion compensates for the dispersion of single-mode fiber (SMF) with shorter length, which can reduce the losses and nonlinearity of the compensation. Therefore, studying DCF with large negative dispersion is substantial.

In this letter, chromatic dispersion property of PCF is studied and optimized for dispersion compensation at wavelength 1550 nm using both geometric and liquid-fill schemes with finite element method (FEM). We change the size of first-layer holes through both the regular method (with center fixed) and the new method (with near-core point fixed) to increase slope difference of index curves between the inner and outer mode. Changing the size of first-layer holes with near-core point fixed affects mode indices less at short wavelengths. This process also reduces the change of couple wavelength. All modes in this letter refer to fundamental modes of PCF. Based from the numerical result, compared with regular changing of the first-layer hole sizes, the new method is found to exert less effects on the index curve of inner mode at short wavelengths than long wavelengths. In addition, the new method shows much less influence on the shift of phase-matching point.

The cross-sectional view of the DC-PCF model considered in the present study is shown in Fig. 1; where d_1 is the first-layer hole diameter, d is the background and ring-core hole diameter (i.e., holes aside from the first-layer holes), and Λ is the hole pitch of the triangle lattice structure. The background material is made of pure silica, whose refractive index can be described using Sellmeier equation[9]:

$$n(\lambda) = \Big[1 + \frac{0.6961663\lambda^2}{\lambda^2 - (0.0684043)} + \frac{0.4079426\lambda^2}{\lambda^2 - (0.1162414)^2} + \frac{0.8974794\lambda^2}{\lambda^2 - (9.896161)^2}\Big]^{\frac{1}{2}}. \tag{2}$$

The solid core is formed by removing a central air hole, and the sixth-layer ring holes that are filled with liquids

(with refractive index $n_R = 1.3069$)[7] form the outer ring core. The background holes are temporarily filled with air (with refractive index $n_b = 1$). The filling material is changed in the following paragraphs.

Filling liquid into specified air holes can be achieved by connecting a DC-PCF to a preformed section before filling the holes. Filling the liquid into the preformed fiber is more convenient than into the microstructured PCF[8].

In Fig. 1, first-layer hole diameter is larger than the rest because increasing the slope difference between the inner and outer mode would cause a large negative dispersion coefficient, which can be seen from Eq. (1). Thus, the main target of optimization is to increase the slope of inner mode index curve and reduce the slope of outer mode index curve. For the mode with a shorter wavelength, its electromagnetic energy mainly concentrates in inner-silica-core region; whereas for the mode with a longer wavelength, the energy expands into the outer-air-hole region. Therefore, enlarging the first-layer hole diameter has larger impact on effective index reduction at long wavelengths than at short wavelengths, as shown in Fig. 2.

Figure 2 shows the dependence of inner mode effective indices on wavelengths for PCFs crystal fibers with different first-layer hole diameters. Enlarging the first-layer

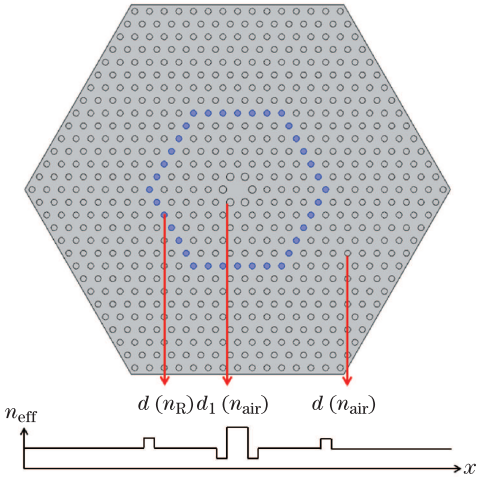

Fig. 1. Cross-sectional view of DC-PCF structure. Λ = 2.4 μm, d= 0.96 μm, d_1 = 1.2 μm, n_R = 1.3069, n_{air} = 1.

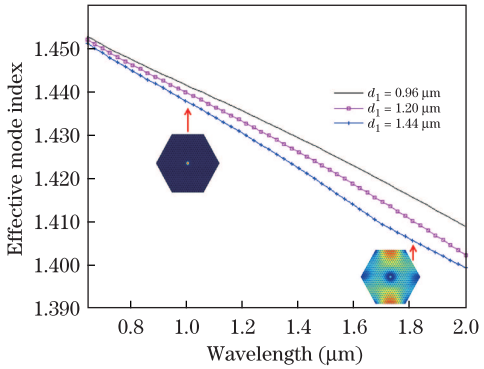

Fig. 2. Dependence of inner mode effective indices on wavelength for PCFs with different first-layer hole diameters.

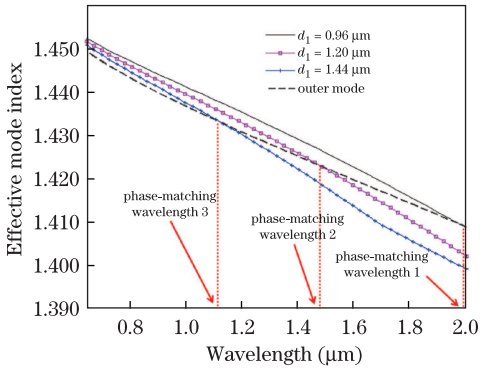

Fig. 3. Variation in phase-matching wavelength with different first layer diameters.

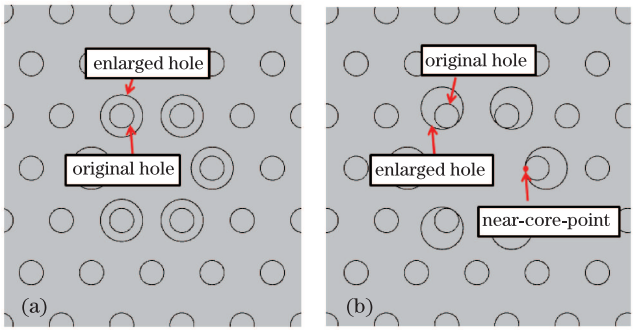

Fig. 4. Two different methods of enlarging the first-layer holes: (a) center fixed (method 1), and (b) near-core-point fixed (method 2).

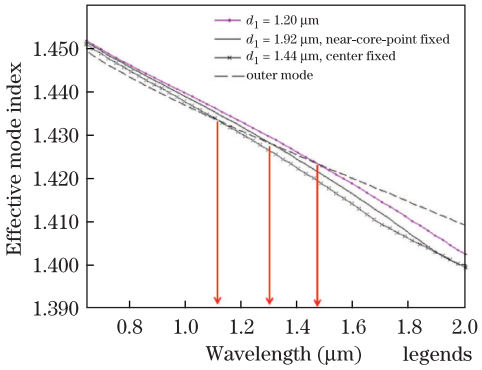

Fig. 5. Effective indices on various wavelengths of: PCF 1: d_1 = 1.2 μm; PCF 2: d_1 enlarged to 1.92 μm with fixed near-core point; PCF 3: d_1 enlarged to 1.44 μm with fixed center. The phase-matching wavelengths are marked with red arrows.

holes is shown to increase the inner mode index curve slope. However, the first-layer hole diameter cannot be simply enlarged without limitation. First, the mode with lower effective index caused by the larger first-layer hole diameter couples with a high-loss cladding mode, which is shown by the cross-sectional view of the PCF electric field in Fig. 2. The inflective point of PCF index curve with d_1 = 1.44 μm at wavelength around 1.65 μm indicates mode coupling into the high-loss cladding region. The coupling is supposed to occur at wavelength longer than the 1.55 μm target phase-matching wavelength. Second, although the size of first-layer holes affects the

indices of longer wavelength more, this parameter also affects the indices of shorter wavelength. This phenomenon causes great irregularity of phase-matching wavelength, as is shown in Fig. 3. To adjust the phase-matching wavelength to 1.55 μm, further work on outer mode is necessary.

Given the abovementioned problems, we enlarge the first-layer holes in a different manner with near-core point fixed (denoted as method 2) instead of center fixed (method 1), as shown in Fig. 4. Enlarging the first-layer holes through method 2 barely affects the core region geometry, as well as the effective index of short wavelength, because light with short wavelength mainly concentrates in the core region. Meanwhile, light with a long wavelength expands into the outer-hole region.

The different effects of these two methods on effective mode indices of the inner mode are shown in Fig. 5. The effective mode index curve of PCF type 2 are close to the index curve of the PCF with unchanged first-layer holes at short wavelengths but moves close to the index curve of PCF type 3 at long wavelengths. This process results in a large slope index curve while the inflective point settles at a longer wavelength. Less effective index change is found at short wavelengths; therefore, the extra work on outer mode to adjust the phase-matching wavelength is reduced.

Figure 6 shows the chromatic dispersion properties of PCF 1: $d_1 = 1.2$ μm, d= 0.94 μm; PCF 2: d_1 enlarged to 1.92 μm with near-core-point fixed, $d = 0.992$ μm; PCF 3: $d1$ enlarged to 1.44 μm with center fixed, $d = 1.05$ μm. PCF 2 and PCF 3 both gain a larger chromatic dispersion value than PCF 1. The chromatic dispersion values of PCF 2 and PCF 3 are close, while the size difference of cladding holes between PCF 2 and PCF 1 (0.052 μm) is much less than the difference between PCF 3 and PCF 1 (0.11 μm), which means less efforts of changing cladding holes' diameter is needed to adjust the phase-matching wavelength.

In this letter, the sixth-layer ring holes filled with liquids form the outer ring core. The distance between central core and ring core affects the PCF dispersion coefficient. If the distance is small, then the guided modes of both cores are strongly coupled, and the effective refractive index of the coupled mode is gradually changed with wavelength resulting in smaller negative dispersion coefficient. By contrast, if the distance is large, then the effective refractive index change of the coupled mode is large around the phase matched wavelength leading to larger negative dispersion coefficient[6]. However, distance cannot be simply enlarged because a large distance also results in difficult coupling between inner and outer modes.

Optimization of outer modes contains reduction of the index-curve slope, and adjustment of the phase-matching wavelength. The index-curve slope reduction of outer modes is based on the same theory that short wavelength light mainly concentrates in silica region, whereas light with long wavelength expand into air-hole region. The main purpose of this process is to increase the effective mode indices at long wavelengths. Reducing the cladding-hole diameter is effective; however, this process counteracts the phase-matching wavelength adjustment. To reduce the slope of outer mode index-curve, the cladding-hole diameter needs to be smaller, whereas a larger cladding-hole diameter is usually needed to adjust the phase-matching wavelength. Filling background holes with material, whose refractive index is higher than air, is proven to be an effective replacement[7−11].

Figure 7 shows the different effects on the effective indices of outer modes by reducing background holes and filling background holes with liquid. The liquid-filling method affects the effective indices more at long wavelengths than hole-diameter reduction method; meanwhile, the effective indices are affected less at short wavelengths.

Optimization of inner core makes the inner mode effective index curve moves down; whereas optimization of ring core makes the outer mode effective index curve moves up. This finding causes the phase-matching wavelength to move to a short wavelength. To adjust the phase-matching wavelength to 1.55 μm, we alter the cladding-hole diameter.

We enlarge first-layer hole diameter to 1.9 μm with center fixed. This diameter is then enlarged to 2.36 μm with near-core-point fixed. The ring-core holes are filled with liquid refractive index $n_R = 1.3069$ and the rest of the background holes are filled with liquid with refractive index $n_b = 1.2$. We resize the background and ring-core holes to 1.414 μm, and hole pitch Λ to 2.3 μm to adjust phase-matching wavelength to 1.55 μm. The chromatic dispersion property of the DC-PCF we proposed is shown

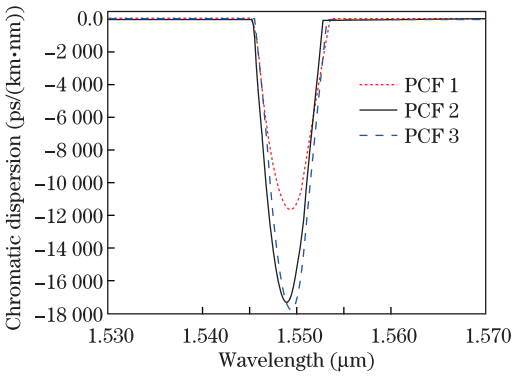

Fig. 6. Chromatic dispersion values of PCF 1: $d_1 = 1.2$ μm, $d = 0.94$ μm; PCF 2: d_1 enlarged to 1.92 μm with fixed near-core point, $d = 0.992$ μm; PCF 3: d_1 enlarged to 1.44 μm with fixed center, $d = 1.05$ μm.

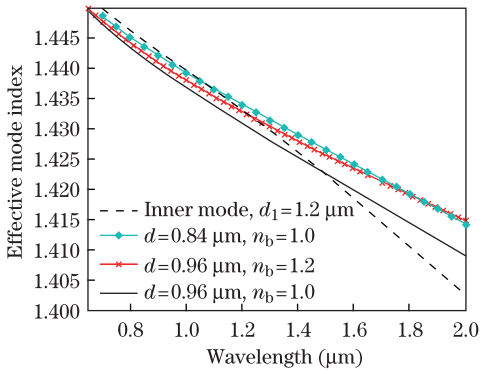

Fig. 7. Effective indices on various wavelengths of outer modes with different d and n_b.

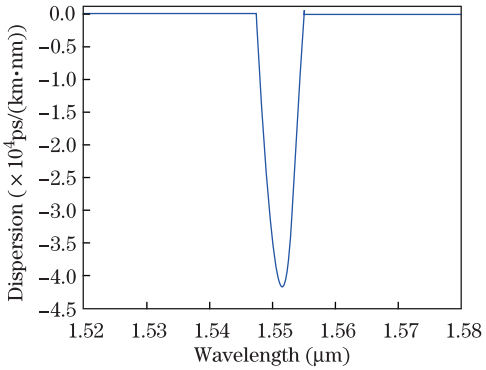

Fig. 8. Chromatic dispersion of DC-PCF: $d_1 = 2.36$ μm with first-layer holes move outward 0.23 μm, $d = 1.414$ μm, $n_R = 1.3069$, $n_b = 1.2$.

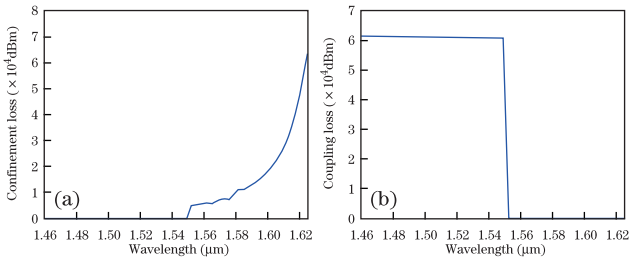

Fig. 9. Characteristics of the proposed DC-PCF: (a) confinement loss, and (b) coupling loss using standard G.655 fibers.

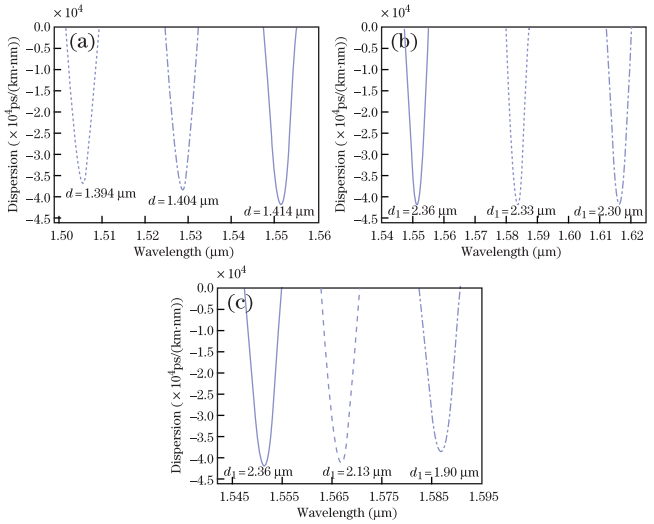

Fig. 10. Influences on phase-matching wavelength of (a) cladding-hole diameter (d), (b) resizing first-layer holes with fixed center, and (c) resizing first-layer holes with fixed near-core point.

in Fig. 8. This DC-PCF shows a negative chromatic dispersion coefficient of approximately –41800 ps/(km·nm) at wavelength around 1550 nm. Figure 9(a) demonstrates the confinement loss of the proposed DC-PCF. Figure 9(b) demonstrates the coupling loss of the proposed DC-PCF with a G.655 fiber. The small effective mode area is at short wavelength; thus, the proposed DC-PCF shows obvious coupling loss. Further work is needed to reduce the coupling loss.

The influences on phase-matching wavelength by changing cladding-hole diameter (d), resizing first-layer holes with center fixed, and resizing with near-core-point fixed are shown in Fig. 10. The factors are fixed as the designed value ($\Lambda = 2.3$ μm; $d = 1.414$ μm; d_1 is enlarged to 1.9 μm with center fixed to 2.36 μm with near-core-point fixed) except for the variant factor. Figure 10(a) demonstrates the influence of different cladding-hole diameters (i.e., 1.394, 1.404, and 1.414 μm). The results match that of the previous discussion. Figures 10(b) and (c) show the influences of changing first-layer hole diameter with center fixed and near-core-point fixed, respectively. The wavelength shift of changing d_1 with near-core-point fixed (about 0.09 μm deviation per μm) is much smaller than changing with center fixed (about 1 μm deviation per μm). We study the effects of first-layer hole size and position, as well as that of cladding-hole size on the chromatic dispersion properties of DC-PCF. We find that by enlarging first-layer holes with near-core-point fixed, less efforts of changing cladding-hole diameter is needed to obtain a large negative dispersion coefficient and adjust the phase-matching wavelength. We propose a DC-PCF, which attained a chromatic dispersion coefficient at approximately –41 800 ps/(km·nm) and approximately 1.55 μm wavelength.

This work was supported by the National "863" Program of China (No. 2013AA031501) and the Fundamental Research Funds for the Central Universities of China (No. 2012RC0402).

References

1. M. Zhang, S. Li, N. Shi, Y. Gu, P. Wu, X. Han, and M. Zhao, Chin. Opt. Lett. **10,** 070602 (2012).
2. K. Mukasa and T. Yagi, in *Proceedings of OFC 2001* TuH7 (2001).
3. J.-L. Auguste, R. Jindal, J.-M. Blondy, M. Clapeau, J. Marcou, B. Dussardier, G. Monnom, D. B. Ostrowsky, B. P. Pal, and K. Thyagarajan, Electron. Lett. **36,** 1689 (2000).
4. F. Gerome, J.-L. Auguste, and J.-M. Blondy, Opt. Lett. **29,** 2725 (2004).
5. W. Liang, N. Liu, Z. Li, and P. Lu, Chin. Opt. Lett. **11,** S20604 (2013).
6. T. Fujisawa, K. Saitoh, K. Wada, and M. Koshiba, Opt. Express **14,** 893 (2006).
7. C. Yu, J. Liou, S. Huang, and H. Chang, Opt. Express **16,** 4443 (2008).
8. J.-M. Hsu and G.-S. Ye, J. Opt. Soc. Am. B **29,** 2021 (2012).
9. I. Malitson, J. Opt. Soc. Am. **55,** 1205 (1965).
10. T. Cheng, M. Liao, W. Gao, Z. Duan, T. Suzuki, and Y. Ohishi, Opt. Fiber Technol. **18,** 498 (2012).
11. Y. Liu, J. Wang, Y. Li, R. Wang, J. Li, and X. Xie, Opt. Laser Technol. **44,** 2076 (2012).